ELSEVIER

Polymer 42 (2001) 2991–3001

polymer

www.elsevier.nl/locate/polymer

Synthesis, characterization and charge transport mechanism in conducting polyaniline/V_2O_5 composites

Prakash R. Somani[a,*], R. Marimuthu[a], A.B. Mandale[b]

[a]*Centre for Materials for Electronics Technology (C-MET), Panchawati, Off Pashan road, Pune 411 008, India*
[b]*Physical Chemistry Division, National Chemical Laboratory, Pune 411 008, India*

Received 7 April 2000; received in revised form 1 September 2000; accepted 5 September 2000

Abstract

Conducting polyaniline/V_2O_5 composites have been synthesized byan 'in situ' deposition technique using the fine-grade powder (average particle size of approximately 400 nm) of V_2O_5 in the polymerization reaction of aniline. The composite thus obtained is studied by physico-chemical characterization techniques such as FTIR spectroscopy, thermal analysis, scanning electron microscopy, and X-ray photoelectron spectroscopy. In addition, the study of the charge transport mechanism reveals that the charge transport is mainly governed by the space charge effects in such a composite. A large hysterisis in the current–voltage (I–V) characteristics, which in turn depend on the composite formation (i.e. the amount of the V_2O_5 added), is also observed.

Keywords: Polyaniline; Conducting polymer composite; Space charge limited conduction

1. Introduction

Conducting polymers have an increasing number of applications in various electronic devices such as chemical sensors, light emitting diodes (LED), electrochromic displays (ECD), and EMI shielding. Among these polymers, polyaniline (PANI) has been studied most extensively in recent years since it can be synthesized easily, is comparatively stable in air, is relatively cheap and exhibits a number of interesting properties such as chemical sensitivity and multicolor electrochromism [1–6].

Conducting polymer composites have attracted considerable interest in the recent years because of their numerous applications in a variety of electric and electronic devices. It has been found that such composites can exhibit some novel properties such as positive temperature coefficient of resistance (PTC), and piezoresistivity [7–10].

Vanadium oxide (V_2O_5) is an interesting material that displays novel properties including electrochromism. The charge storage behavior of deposits of hydrated V_2O_5 is of special interest in rechargeable lithium batteries. In earlier studies, the polymeric chains of polypyrrole (Ppy) and PANI have been interleaved between V_2O_5 sheets by an 'in situ' intercalation and oxidative polymerization methods [11–20]. In this paper, it is proposed to prepare and study the conducting PANI/V_2O_5 composites. The charge transport mechanism in such composites is important and can even be the rate determining factor in many important phenomenona. So, a detailed study of the charge transport mechanism in conducting PANI/V_2O_5 composite is carried out, which reveals a non-linear, space charge limited conduction mechanism (SCLC). In addition, it has been observed that, at high polymer content, these materials show improved conductivity compared to pristine V_2O_5.

2. Experimental

V_2O_5 powder in fine particle form (average particle size approximately 400 nm) was used for the preparation of the composite. In a typical procedure, 10 ml aniline was dissolved in 150 ml distilled water containing 10 ml hydrochloric acid. The solution was precooled to 0°C and the desired quantity of V_2O_5 (ranging from 0 to 10 g) was added to the solution and stirred thoroughly. $(NH_4)_2S_2O_8$ was added to the reaction mixture in the form of aqueous solution (5.4 g dissolved in 30 ml) so that the total volume of the reaction mixture was 200 ml. This was stirred for 30 min and allowed to stand for a further period of 60 min. The resultant product was filtered, washed thoroughly with water and dried till it showed constant weight at 40°C. The resultant powder was analyzed for

* Corresponding author. Tel.: +91-20-5899273; fax: +91-20-5898180.
E-mail address: prsomani@cmetp.ernet.in (P. Somani).

0032-3861/01/$ - see front matter
PII: S0032-3861(00)00670-4

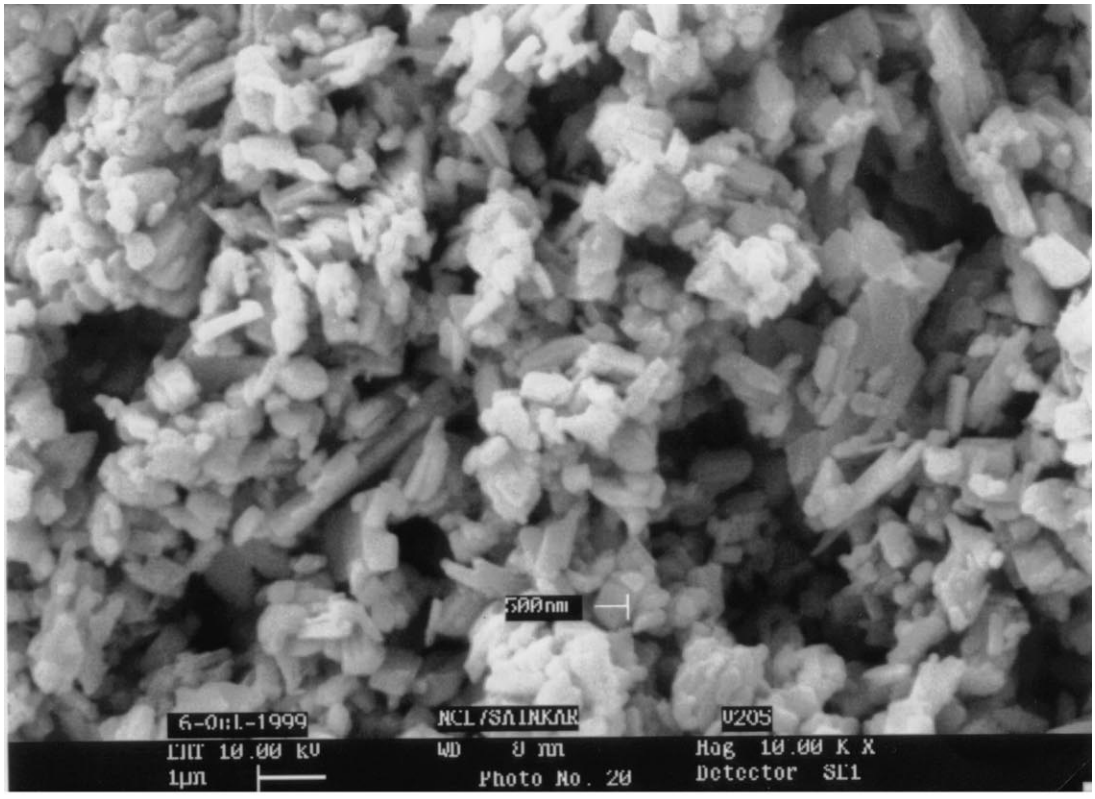

(a)

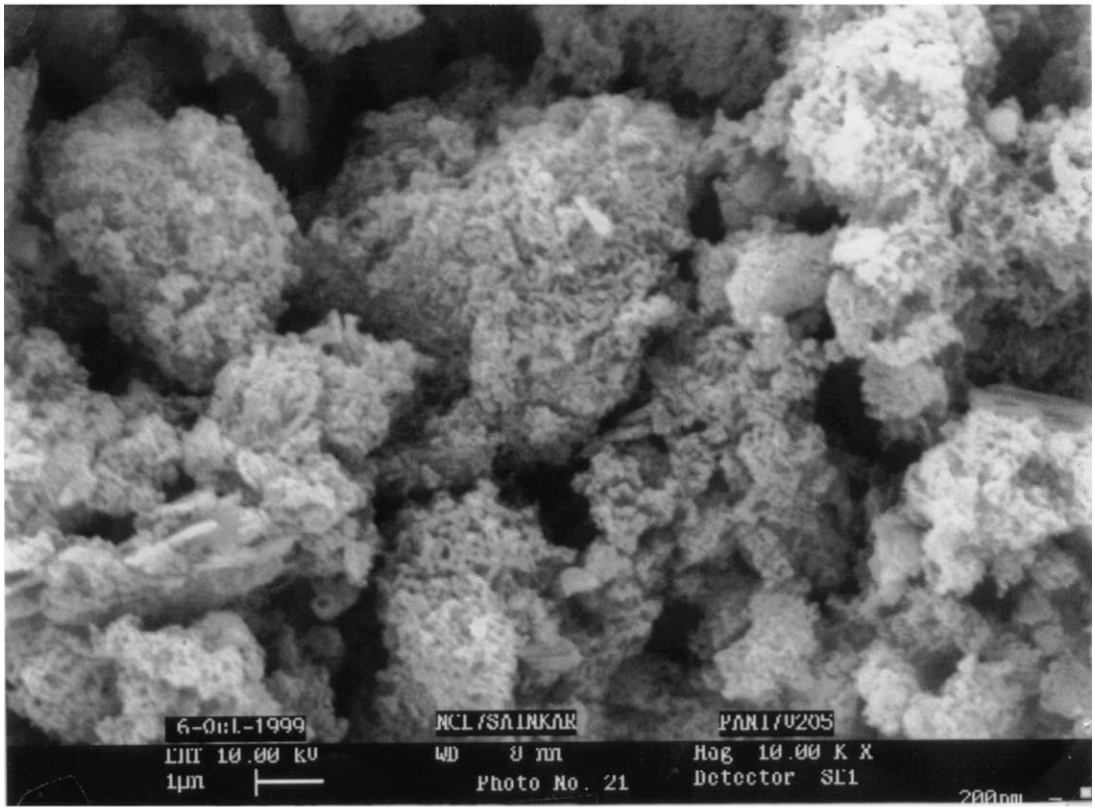

(b)

Fig. 1. SEM micrographs of the: (a) V_2O_5 particles only (showing an average particle size of approximately 400 nm); (b) V_2O_5/PANI composite showing an increase in the particle size from 400 nm (for pure V_2O_5) to 4 μm upon composite formation with PANI.

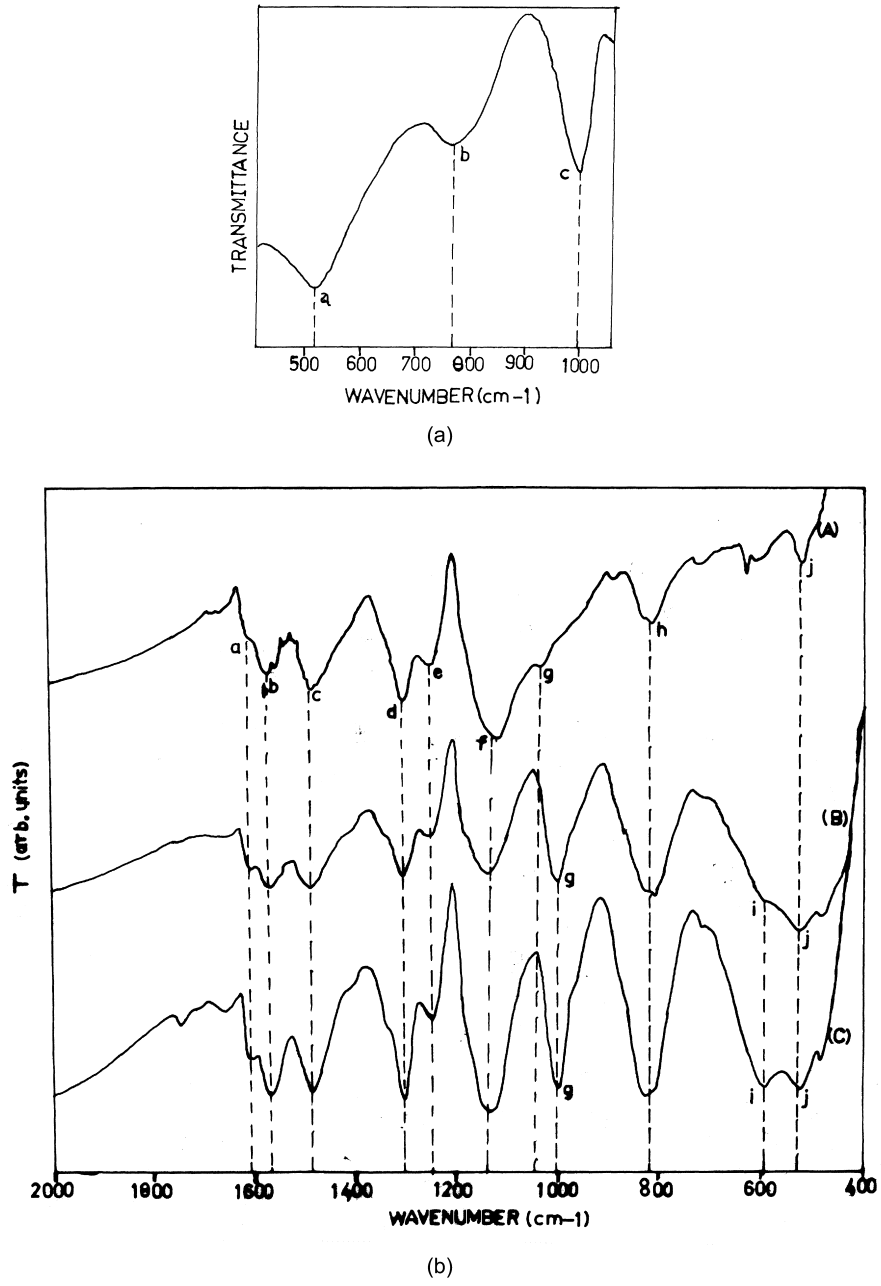

Fig. 2. FTIR spectra of the: (A) V_2O_5 only in the region of interest; (B) V_2O_5/PANI composite with increasing V_2O_5 composition — (a) 17, (b) 28.6 and (c) 38.5 wt.% V_2O_5, respectively.

particle size by scanning electron microscopy (SEM) and for composition and other properties by suitable physico-chemical characterization techniques such as thermogravometric analysis (TGA), differential thermal analysis (DTA), and infrared spectroscopy (FTIR).

The PANI, V_2O_5 and V_2O_5/PANI composite samples prepared were studied by SEM using a SEM Leica stereoscan model 440 manufactured by M/s Leica, Cambridge, UK. For comparative purposes, the electron beam parameters were kept constant while all the samples were analyzed. The micrographs of the samples with 20 kV EHT and 25 pA beam current were recorded using a 35-mm camera attached to the high-resolution recording unit.

The FTIR spectra were recorded on a Perkin Elmer FTIR spectrophotometer model 2000.

The thermal studies of the materials were carried out by recording the thermograms on a TGA/SDTA 851 [e]Mettler Toledo model under a nitrogen atmosphere in a temperature range of 30–950°C at a heating rate of 10°C/min. The DSC studies of the samples were carried out using DSC 821 [e]Mettler Toledo model under a nitrogen atmosphere at a temperature of 550°C and a heating rate of 10°C/min.

X-ray photoelectron spectroscopic (XPS or ESCA) studies of the pure V_2O_5, pure PANI and V_2O_5/PANI composites were carried out on a V.G. Scientific ESCA-3-MK-2 electron spectrometer with an MgKα X-ray source (non-monochromatic). For the present measurements, the anode was operated at 140 W (14 kV, 10 mA) and the analyzer was operated at a constant pass energy of 50 eV. All the spectra were recorded with similar spectroscopic parameters. The binding energy (BE) scale was calibrated by determining the BE of Au $4f_{7/2}$ (84 eV), Ag $3d_{3/2}$ (368.4 eV) and Cu $2P_{3/2}$ (932.4 eV) levels using spectroscopcally pure metals from Johnson–Matthey, London. The BE values (measured to an accuracy of 0.2 eV) are in good agreement with the literature values. The resolution in terms of the full width at half maximum (FWHM) of the Au $4f_{7/2}$ level is 1.6 eV.

A small quantity (0.3 g) of the powder was compacted at 3000 kg/cm^2 pressure in order to prepare thin disc specimens for electrical measurements. The current–voltage (I–V) characteristics were measured using silver and aluminum as the electrodes. The details of these measurements have been described elsewhere.

3. Results and discussion

3.1. SEM analysis

The average particle size as determined by SEM for the pure V_2O_5 particles was about 350 nm, increasing to about 1–4 μm depending on the quantity of PANI formed during the polymerization reaction. Fig. 1a shows the typical SEM micrograph obtained for pure V_2O_5 particles and Fig. 1b displays the micrograph of the V_2O_5/PANI composite.

Table 1
Polyaniline peaks in IR absorption spectra

Assignment	Wavenumber (cm^{-1})	
C–N stretching + C–C stretching	1288–1214	
C–N $^+$stretching + C–C stretching	1228–1221	
C=N stretching + C–C stretching	1522–1480	
C–N + stretching + C–C stretching	1401–1383	
	Benzenoid	Quinoid
Aromatic Ring	1625–1615	1580–1590
	840–820	780–810
CH (ip) bending	1185–1175	1160–1180
CH (op)	885–870	
NH stretching	3400–3100	
NH_2^+	3000–2450	
CH (op)	822–810	780–800
Ring stretching	1540–1495	1540–1570
CN stretching + CH bending	1315–1285	1290–1300

3.2. FTIR analysis

Fig. 2A shows the FTIR spectra of pure V_2O_5 only (in the range of interest). Fig. 2B shows the FTIR spectra of the PANI/V_2O_5 composite taken in KBr pallets in dry state. Fig. 2B(a)–(c) represents the PANI/V_2O_5 composites with increasing V_2O_5 composition.

The FTIR spectra of the PANI/V_2O_5 composite between 400 and 2000 cm^{-1} display strong bands in the region 750–1800 cm^{-1} that are characteristics of PANI. Their position and intensity show that the conductive form of the polymer has been produced. The bands also exhibit slight shifts from those of bulk, p-doped PANI, suggesting that a substantial interaction of the polymer with V_2O_5 occurs. More insight into the nature of these interactions is provided by examining the changes occurring in the vibrational modes of the inorganic lattice which dominate the spectrum.

The peaks in the IR absorption spectra of PANI and V_2O_5 (individually) are given in Tables 1 and 2, respectively (see also Ref. [26]. The peaks in the IR absorption spectra of the

Table 2
IR peak positions of V_2O_5

Assignment	Wavenumber (cm^{-1})
$\nu_{\text{symm (V–O–V)}}$	521
$\nu_{\text{asymm (V–O–V)}}$	772
$\nu_{\text{(V=O)}}$	1000

Table 3
IR peak positions in V_2O_5/PANI composite

Wavenumber (cm^{-1})		Assignment
1630	H_2O	
1570	PANI	Ring stretching
1485	PANI	C=N stretching + C–C stretching
1300	PANI	C–N stretching + CH bending
1250	PANI	C–N stretching + C–C stretching
1145	PANI	CH (ip) bending
1000	V_2O_5	$\nu_{\text{(V=O)}}$
810–825	PANI and V_2O_5	Aromatic ring and $\nu_{\text{asymm (V–O–V)}}$
585	V_2O_5	$\nu_{\text{symm (V–O–V)}}$

Table 4
Shifts of the V_2O_5 peaks upon composite formation with polyaniline

Assignment	In V_2O_5 only (cm^{-1})	In V_2O_5/PANI composite (cm^{-1})
$\nu_{\text{symm (V–O–V)}}$	521	585
$\nu_{\text{asymm (V–O–V)}}$	772	810
$\nu_{\text{(V=O)}}$	1000	1050 — for low V_2O_5 content and 1000 — for high V_2O_5 content

PANI/V_2O_5 composite are given in Table 3. Table 4 displays the shifts of V_2O_5 peaks upon composite formation with PANI.

Due to the presence of V–O–V units, two vibrational modes — the symmetric stretch ($\nu_{sym.}$) and the asymmetric stretch ($\nu_{asym.}$) — are expected to occur in the vibrational spectrum in the range 400–800 cm^{-1}. As the symmetric stretch of the M–O–M containing structures usually occurs around 520 cm^{-1}, the peak at 520 cm^{-1} is assigned to the symmetric vibration ($\nu_{sym.}$). A low intensity peak at 772 cm^{-1} is tentatively assigned as ($\nu_{asym.}$), whereas the peak at around 1000 cm^{-1} is assigned to V=O vibration. The assignment of these modes was used to characterize the structural changes associated with the PANI interaction with V_2O_5. We found that both modes shift to higher wavenumbers upon interaction with PANI. The symmetric mode ($\nu_{sym.}$) at 521 cm^{-1} is increased to 585 cm^{-1}. The data suggest a highly interacting PANI/V_2O_5 composite system, in which the coordination environment at the metal center is affected by the interaction with the organic component.

Prior studies on V_2O_5 reported by Savariault et al. with pyridine as the intercalent resulted in lowered frequencies of the V_2O_5 modes in the 500–800 cm^{-1} region [21]. The downshifts were ascribed to the coordination of the pyridine to vanadium ions, which leads to the weakening of the V–O–V bonds. Similar downshifts have also been observed with anilinium ion as a dopant [22]. Our data show that the interaction of the PANI with V_2O_5 has a different nature, leading to different structural perturbation of the oxide.

The vanadium stretch ($\nu_{V=O}$) that occurs at 1000 cm^{-1} shifts to a higher wavenumber, i.e. to 1050 cm^{-1}, for low V_2O_5 content in the composite, but for high V_2O_5 content in the composite it remains only at 1000 cm^{-1}. This implies that when V_2O_5 content is low, the vanadium stretch ($\nu_{V=O}$) i.e. V=O bond is strongly affected (becomes strengthened) by the presence of PANI, whereas when the PANI content in the composite becomes low, there is a negligible effect of PANI on the vanadium stretch. Previous studies on the intercalation of N-containing species indicate that the V–O–V modes are downshifted upon introduction of the guest species. Here, the observed upshifts of both the vibrational modes i.e. $\nu_{sym.}$ and $\nu_{asym.}$ on the composite formation are consistent with the increased bond strengths of the V–O–V groups in the composite. This can be attributed to the increased V^{4+} content in the composite material as a result of reaction with the aniline monomer.

3.3. Thermal analysis

Fig. 3A shows the TGA curve for the PANI only. The initial weight loss (below 150°C) is due to the loss of water/moisture from the polymer. The polymer is thermally stable up to 250°C. After this temperature, the polymer starts to degrade slowly. Above 610°C, the polymer degrades rapidly. Fig. 3b displays the TGA curve for V_2O_5 only. The material is quite stable and does not show any weight loss till 600°C. Fig. 3c shows the TGA curve for the V_2O_5/PANI composite. Curves (A)–(C) represent the increasing quantity of V_2O_5 in the composite. The initial weight loss (below 100°C) can be attributed to the loss of moisture/water (and also the volatile components such as the adsorbed gases) from the composite. Thereafter, sample (A) remains quite stable up to around 250°C. We will call this temperature "critical temperature" and will denote it by T_{crit}. Above this temperature, the composite (mainly polymer) starts to loose its weight slowly, up to 650°C. Above 650°C, the composite starts to degrade very fast. The weight loss above 650°C can be attributed to the combined weight loss of the polymer and of V_2O_5. With an increasing concentration of V_2O_5 in the composite, the critical temperature becomes higher. This means that as the quantity of V_2O_5 in the composite increases, the material becomes more and more stable, i.e. V_2O_5 is not allowing the polymer to degrade very fast. This is simply due to the fact that here V_2O_5 and PANI are directly reacting (redox reacting) with each other and forming a unique organic–inorganic hybrid composite system (as confirmed from the other characterization techniques such as XPS and FTIR). For samples (B) and (C), the critical temperature is approximately 300 and 350°C, respectively, as seen from the graphs. This indicates that V_2O_5 is actually taking part in the chemical polymerization reaction of aniline to form PANI. Actually, the nitrogen (present on PANI) is forming a bond with the oxygen atoms present on V_2O_5 and thus it does not allow the polymer to degrade easily. The higher the quantity of V_2O_5, stronger the bond and hence the sample will show less degradation (i.e. will be more stable with respect to temperature).

Fig. 4a shows the DSC curves for V_2O_5 and PANI, respectively. V_2O_5 does not show any exothermic/endothermic peaks, indicating that there are no physical changes in the sample. The PANI shows two endothermic peaks at around 78 and 245°C, which can be attributed to the expulsion of water/moisture and the thermal degradation of the polymer. Fig. 4b shows the DSC curve for the V_2O_5/PANI composite. It displays two endothermic peaks at around 85 and 345°C. The endothermic peak at around 85°C can be assigned to the expulsion of moisture from the sample. The second endothermic peak at around 345°C is due to the thermal degradation of the composite material.

3.4. XPS analysis

Fig. 5A shows the XPS spectra of the vanadium ($2P_{3/2}$ level) in V_2O_5. The peak of the vanadium $2P_{3/2}$ level occurs at about 517.6 eV. Fig. 5B shows the XPS spectra of the vanadium ($2P_{3/2}$ level) in the V_2O_5/PANI composite. The peak of the vanadium $2P_{3/2}$ level occurs at about 516.6 eV.

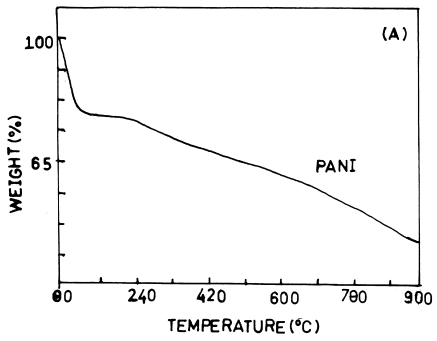

(a)

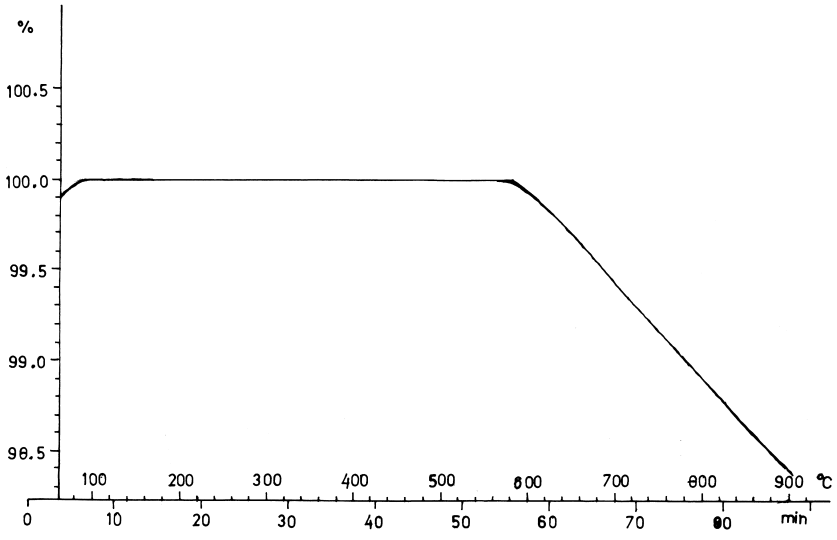

(b)

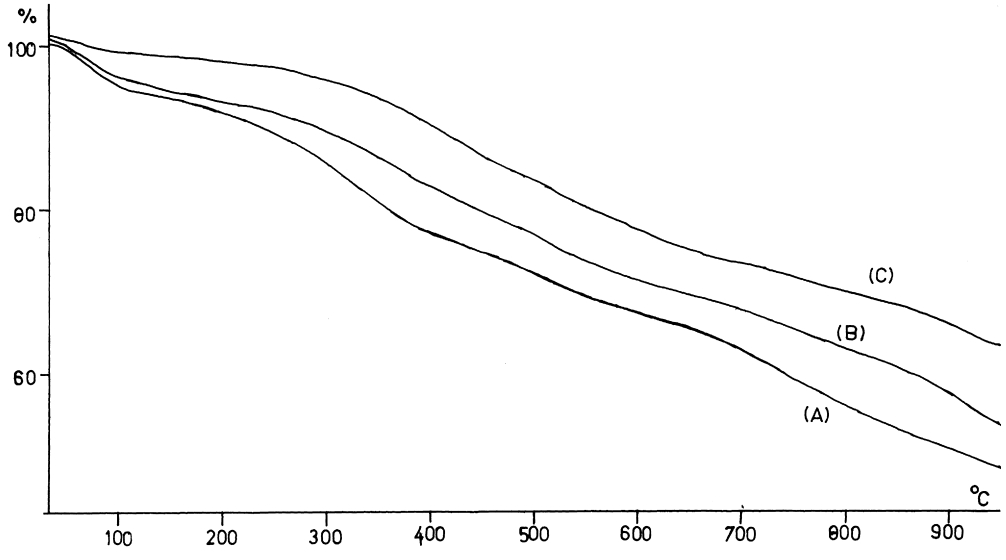

(c)

Fig. 3. TGA curves for the: (A) PANI; (B) V_2O_5; (C) V_2O_5/PANI composites (containing (a) 83, (b) 71.4, and (c) 62.5 wt. % PANI).

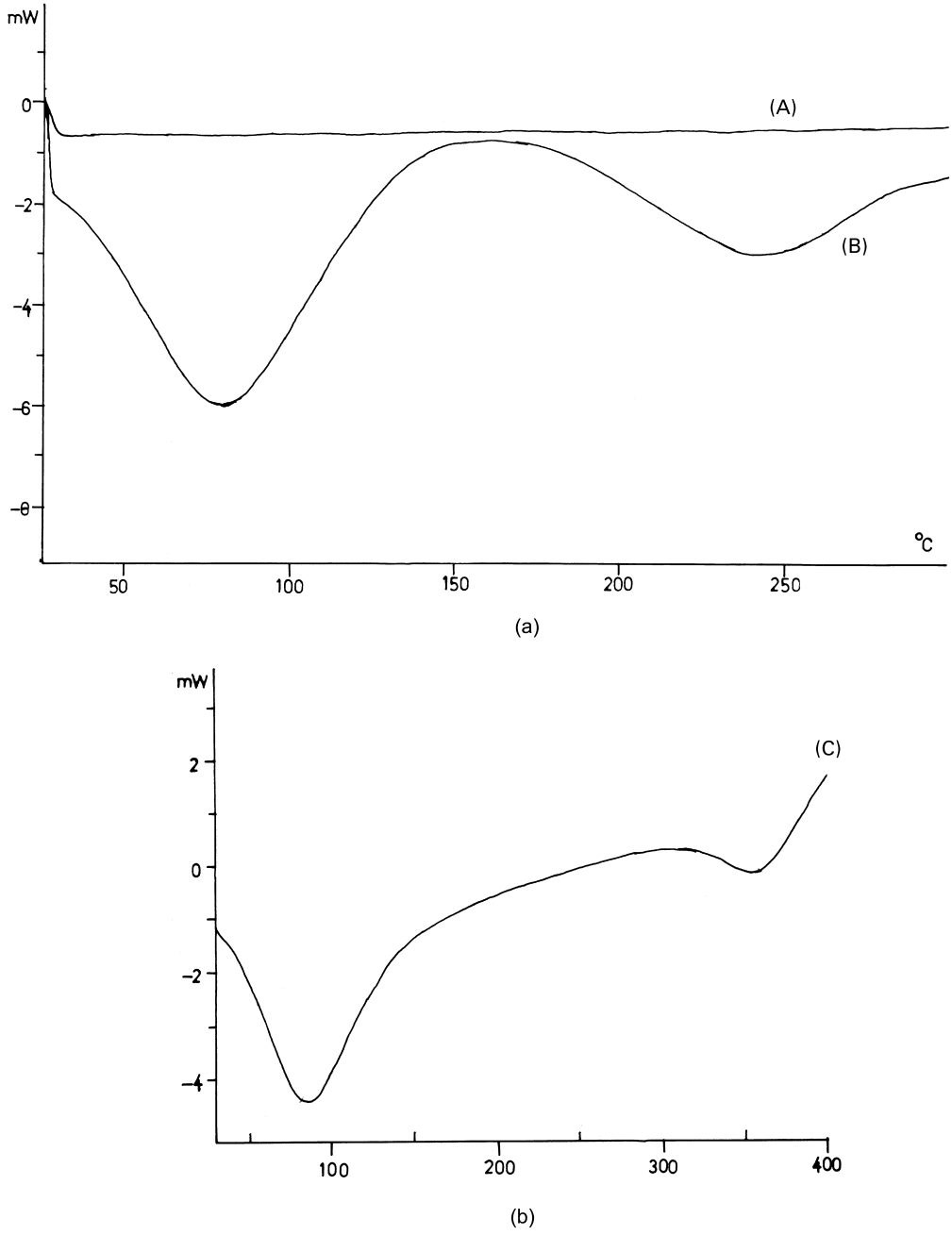

Fig. 4. DSC curves for the: (A) V_2O_5; (B) PANI; (C) V_2O_5/PANI (71.4 and 28.6 wt.% V_2O_5).

Thus, it can be seen that the peak position of the vanadium $2P_{3/2}$ level shifts to the lower BE side (by about 1 eV) upon formation of the composite with PANI. Thus, the vanadium is getting converted to the lower oxidation state (in other words, it is getting reduced). It can be said that the V_2O_5 is reduced. Hence, the oxidative polymerization of the aniline to form PANI in presence of V_2O_5 is a redox reaction in which the aniline monomer is oxidatively polymerized and the V_2O_5 is reduced generating V^{4+} centers and thus forming a united electronic (organic–inorganic hybrid composite) system. The redox reaction can be represented as

$$n\,(\text{aniline monomer}) + n(V_2O_5) \xrightarrow[HCl]{(NH_4)_2S_2O_8} \text{polyaniline} + n(V_2O_5)^-$$

Fig. 6A shows the XPS spectra of the nitrogen (1S level) in PANI only. There are two peaks centered at around 868.0 eV (marked as I) and 870.6 eV (marked as II). Fig. 6B displays the XPS spectra of the nitrogen (1S level) in the V_2O_5/PANI composite. There are two broad peaks centered

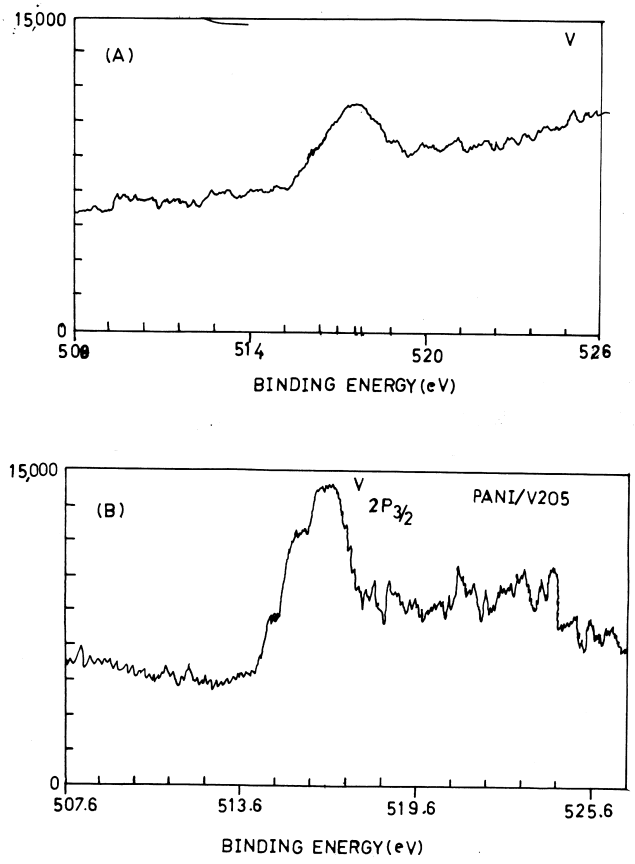

Fig. 5. XPS spectra of vanadium $2P_{3/2}$ level in: (A) V_2O_5; (B) V_2O_5/PANI (28.6 wt.%/71.4 wt.%) composite.

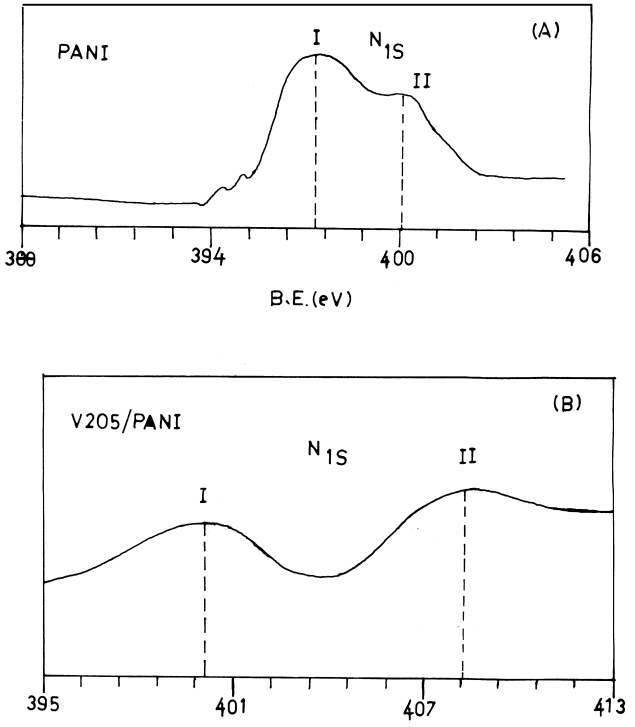

Fig. 6. XPS spectra of the nitrogen 1S level in: (A) PANI; (B) V_2O_5/PANI (28.6 wt.%/71.4 wt.%) composite.

at about 870.0 eV (marked as I) and 878.4 eV (marked as II). Thus, it can be seen that there are two peaks of nitrogen (in PANI) which shift to the higher BE side by about 2 and 8.2 eV, respectively. The shifting of the nitrogen 1S level peaks to the higher BE side is presumably due to the strong interaction and the (ONO_2) type bond formation of the nitrogen with the oxygen atoms of the V_2O_5 [23]. In addition, it can be seen that the second peak (marked as II), which is just a hump in PANI, gets converted into a separate broad peak. The upshift in the BE value of the nitrogen 1S peak (marked as II) is very high (about 8.2 eV). Hence, this signal (second peak) must be coming from the nitrogen atoms which are strongly interacting (and which are in immediate contact with the V_2O_5 surface) with the V_2O_5.

Fig. 7A represents the XPS spectra of the oxygen (1S level) in V_2O_5 only. The broad peak, which is centered at

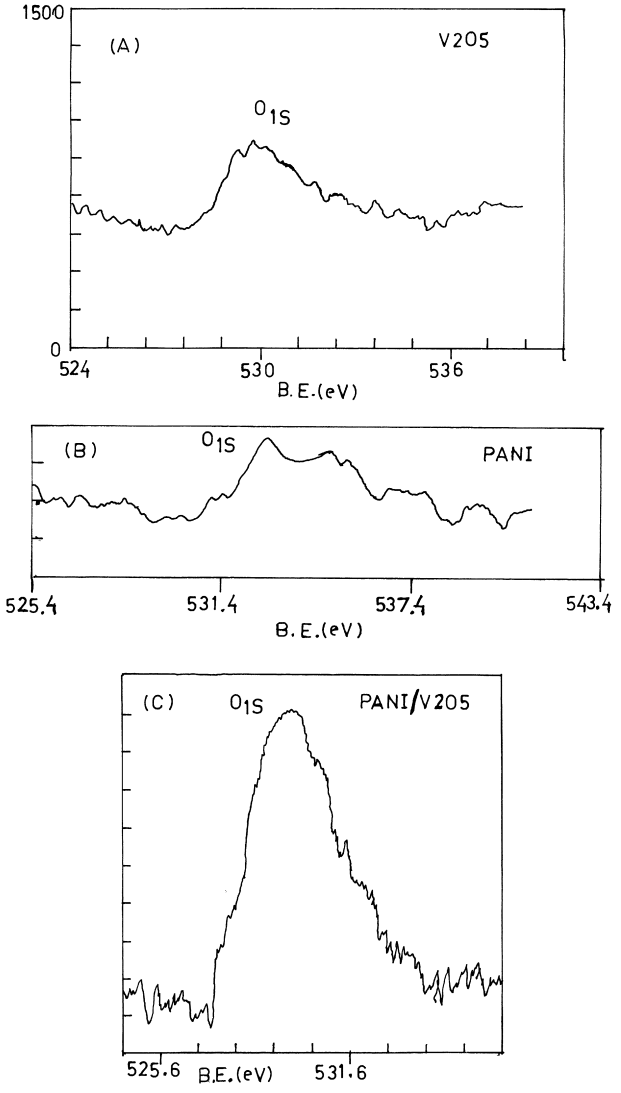

Fig. 7. XPS spectra of the oxygen 1S level or vanadium $2P_{1/2}$ level in V_2O_5 (A); XPS oxygen 1S level in PANI only (B) and oxygen 1S level and vanadium $2P_{1/2}$ level in V_2O_5/PANI (28.6 wt.%/71.4 wt.%) composite.

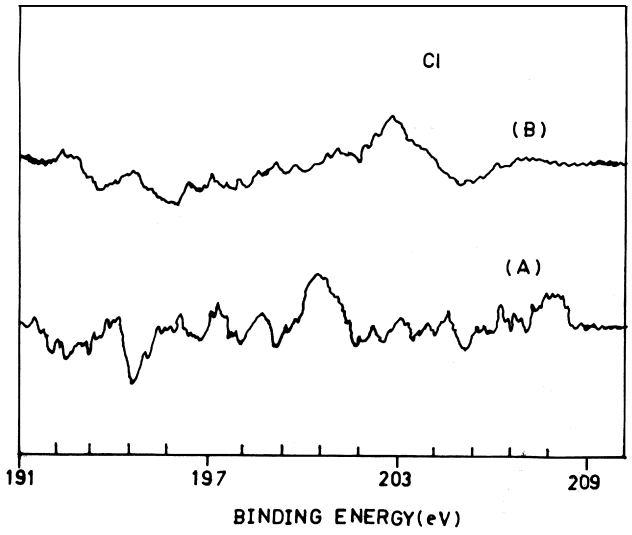

Fig. 8. XPS spectra of the Cl^- in (A) PANI; and that in (B) V_2O_5/PANI (28.6 wt.%/71.4 wt.%) composite.

about 529.8 eV, can be resolved into two peaks centered at around 529.4 and 530.6 eV, respectively, and can be assigned to the adsorbed oxygen and lattice oxygen, respectively. Fig. 7B shows the XPS spectra of the oxygen (1S level) in PANI. There are two broad peaks centered at around 532.6 and 535.0 eV, which can be attributed to the adsorbed oxygen and the lattice oxygen (from the moisture/water usually present in PANI) from the polymer. Fig. 7C displays the XPS spectra of the oxygen (1S level) in the V_2O_5/PANI composite. The peak is centered at about 529.2 eV and is very broad, due to the fact that this signal will come from both the V_2O_5 and the PANI lattice.

Fig. 8A and B represents the XPS spectra of the Cl in PANI and in the V_2O_5/PANI composite, respectively. It can be seen that the peak position of Cl shifts to the lower BE side in the composite by approximately 2.5 eV. Actually while chemical polymerization of aniline to form PANI takes place, we are intercalating Cl^- into the backbone of PANI. This Cl^- usually associates with the nitrogen present on PANI. Here, the nitrogen on PANI itself forms a bond with the oxygen on V_2O_5, the bond between the nitrogen on PANI and Cl^- dopant weakens in the composite and thus the XPS spectra of Cl shifts to the lower BE side.

3.5. Charge transport mechanism

Fig. 9 shows the typical *I–V* characteristics curves of the PANI/V_2O_5 composite between the silver and aluminum electrodes. It indicates a typical Schottky diode type behavior, which is attributable to the fact that silver is forming an ohmic contact while aluminum forms a blocking contact with the composite under study. In the first quadrant, silver is positive while in the third quadrant, silver is negative. The curve is recorded continuously and the readings are taken instantaneously under a minimum pressure of 50 g/cm^2 to ensure a good press contact of the upper aluminum electrode. By comparison, it can be seen from the current values that as the V_2O_5 content in the composite increases, the sample becomes more and more non-conducting. Detailed analysis of the current–voltage (*I–V*) characteristic curves reveals that the charge transport is mainly governed by the SCLC process. In such cases, the current–voltage relationship is given in Refs. [24,25]

$$I = 9/8\mu\Theta\{V^{(n+1)}/d^{(2n+1)}\} \quad (1)$$

where μ is the mobility of the charge carriers, Θ a

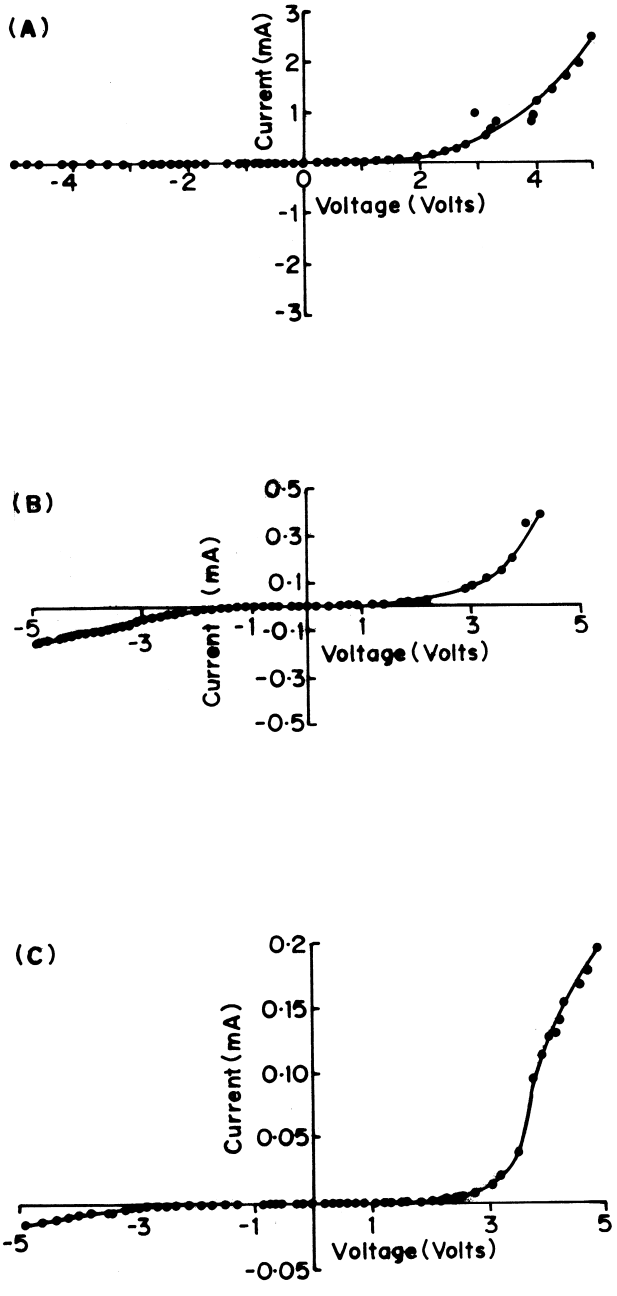

Fig. 9. *I–V* characteristics of the V_2O_5/PANI composite containing increasing amount of V_2O_5: (A) 17, (B) 28.6 and (C) 38.5 wt.%.

parameter depending on concentration of the trapping/impurity centers and their distribution, V the voltage applied, d the interparticulate distance and n an integer ($n \geq 1$). The above relationship was confirmed by the plot of the current–voltage (I–V) characteristics on a log–log scale (as shown in Fig. 10). The I–V characteristics on the log–log scale are linear with two slopes, i.e 1 in the low-voltage region and 2–3 in the high-voltage region. The critical voltage at which the curve passes from the ohmic to the non-ohmic region is given in Refs. [24,25]

$$V_{\text{crit.}} = 8/9\{d^{(2n)}/\Theta\mu\} \quad (2)$$

As the V_2O_5 content in the composite increases, the value of the $V_{\text{crit.}}$ shifts to high voltage side and the curve becomes more and more non-linear. One of the most important features of the space charge effect is the trapping and accumulation of the charge in the material. The hysterisis in the I–V characteristics clearly implies charge storage in the sample (hysterisis curves are not shown here). In the present case, the charge would be accumulated at the interface between PANI and V_2O_5.

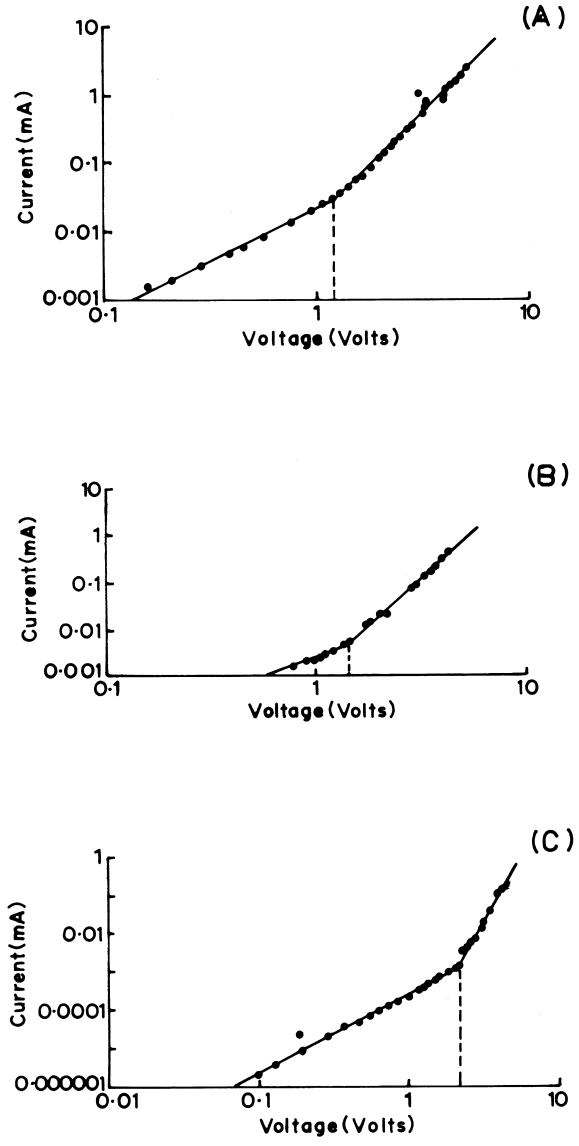

Fig. 10. I–V characteristics of the V_2O_5/PANI composites as considered earlier on the log–log scale indicating the non-linear SCLC type charge transport mechanism.

4. Summary and conclusions

Conducting polyaniline (PANI)/V_2O_5 composites have been synthesized by an in situ deposition technique. The dispersed V_2O_5 particles remain intact and preferentially on the surface, where the polymerization of aniline to form PNI occurs. The aniline is oxidatively polymerized to yield PANI (in the oxidized form, due to the addition of the intercalents) and at the same time V_2O_5 is reduced (as conformed by the X-ray photoelectron spectroscopy and also supported by the IR measurements) to form a unique organic–inorganic hybrid composite system. In addition, thermal analysis of this composite system shows that V_2O_5 is indirectly taking part in the chemical polymerization reaction of aniline to form PANI. The current–voltage (I–V) characteristics in such composites reveal that the charge transport is mainly governed by the space charge effects (occurring at the interface of the conducting PANI and V_2O_5). A large hysterisis in the I–V characteristics was found, which also supports the SCLC type charge transport mechanism. At high polymer content in the composite, these materials show improved conductivity as compared to the pristine V_2O_5.

References

[1] Petty MC, Bryce MR, Bloor D. An introduction to molecular electronics. London: Edward Arnold, 1995.
[2] Scrosati B. Applications of electroactive polymers. London: Chapman and Hall, 1993.
[3] Alcacer L. Conducting polymers — special applications. Dordrecht: Reidel, 1989.
[4] Epstein AJ, Mac Diarmid AG. Makromol Chem, Macromol Symp 1991;51:217.
[5] Heinze J. Top Curr Chem 1990;2:152.
[6] Yang Y, Heeger AJ. Appl Phys Lett 1994;64:1245.
[7] Somani P, Marimuthu R, Mulik UP, Sainkar SR, Amalnerkar DP. Synth Met 1999;106:45–52.
[8] Somani P, Radhakrishnan S. Chem Phys Lett 1998;292:218–22.
[9] Somani P, Kale BB, Amalnerkar DP. Synth Met 1999;106:53–58.
[10] Somani P, Mandale AB, Radhakrishnan S. Acta Mater 2000;48(11):2859–71.
[11] Burke LD, O'Sullivan EJM. J Electroanal Chem 1980;111:383–4.
[12] Kanatzidis MG, Tonge LM, Marks TJ. J Am Chem Soc 1987;109:3797–9.
[13] Kanatzidis MG, Wu C-G. J Am Chem Soc 1989;111:4139–41.
[14] Wong HP, Dave BC, Leroux F, Harreld F, Dunn B, Nazar LF. J Mater Chem 1998;8(4):1019–27.
[15] Wu C-G, Liu Y-C, Hsu S-S. Synth Met 1999;102(1–3):1268–9.
[16] Lira-Cantu M, Gomez-Romero P. J New Mater Electrochem Syst 1999;2(2):141–4.

[17] Lira-Cantu M, Gomez-Romero P. J Electrochem Soc 1999; 146(6):2029–33.
[18] Pokhodenko VD, Krylov VA, Kurys YI, Posudievsky OY. Phys Chem Chem Phys 1999;15:905–8.
[19] Lira-Cantu M, Geomez-Romero P. Recent Res. Dev. Phys. Chem. 1997;1:379–401.
[20] Kuwabata S, Idzu T, Martin CR, Yoneyama H. J Electrochem Soc 1998;145(8):2707–10.
[21] Savariault JM, Lafargue D, Parise JL, Galy J. J Solid State Chem 1992;97:169.
[22] Liu YJ, DeDeGroot DC, Schindler JL, Kannewarf CR, Kanatzidis MG. J Chem Soc, Chem Commun 1993:593.
[23] Briggs D, Seah MP. Practical surface analysis by Auger and XPS. London: Wiley, 1984.
[24] Gutman F, Lyons LE. Organic semiconductors. New Work: Wiley, 1967.
[25] Senor DA. Electrical properties of polymers. New York: Academic Press, 1982.
[26] Trivedi DC. In: Nalva HS, editor. Handbook of organic conductive molecules and polymers. New York: Wiley, 1997. p. 537.